JB
Journals.ASM.org

A Clp/Hsp100 Chaperone Functions in *Myxococcus xanthus* Sporulation and Self-Organization

Jinyuan Yan, Anthony G. Garza, Michael D. Bradley, and Roy D. Welch

Department of Biology, Syracuse University, Syracuse, New York, USA

The Clp/Hsp100 proteins are chaperones that play a role in protein degradation and reactivation. In bacteria, they exhibit a high degree of pleiotropy, affecting both individual and multicellular phenotypes. In this article, we present the first characterization of a Clp/Hsp100 homolog in *Myxococcus xanthus* (MXAN_4832 gene locus). Deletion of MXAN_4832 causes defects in both swarming and aggregation related to cell motility and the production of fibrils, which are an important component of the extracellular matrix of a swarm. The deletion also affects the formation of myxospores during development, causing them to become sensitive to heat. The protein product of MXAN_4832 can act as a chaperone *in vitro*, providing biochemical evidence in support of our hypothesis that MXAN_4832 is a functional Clp/Hsp100 homolog. There are a total of 12 Clp/Hsp100 homologs in *M. xanthus*, including MXAN_4832, and, based on its mutational and biochemical characterization, they may well represent an important group.

The Clp/Hsp100 proteins are ubiquitous among bacteria, lower eukaryotes, and plants. At the molecular level, Clp/Hsp100 proteins are all thought to be chaperones that function as protein reactivators and/or degradation partners (8, 12). At the cellular level, the function of Clp/Hsp100 proteins is complicated, as evidenced by the fact that these proteins exhibit a high degree of pleiotropy (25). For example, in *Bacillus subtilis*, the Clp/Hsp100 family member ClpC was found to regulate genetic competence (17), whereas, in the pathogen *Listeria monocytogenes*, a ClpC paralog is involved in escaping from phagosomes (23, 24) and in host cell adhesion and invasion (21). This pleiotropy has been observed not only between species but also between Clp/Hsp100 homologs within the same species; a second Clp/Hsp100 homolog in *L. monocytogenes*, ClpE, is involved in both virulence and cell division (20). From the accumulated data, it seems logical to postulate that members of the Clp/Hsp100 family of proteins function both in a bacterial cell's individual cellular processes and in its interactions with the environment.

No Clp/Hsp100 protein has been characterized in the multicellular prokaryote *Myxococcus xanthus*, even though there are ample opportunities for these proteins to play a role in its complex response to starvation stress. On nutrient-rich agar, *M. xanthus* grows as a single-species biofilm called a swarm. On nonnutritive (starvation) agar, a swarm does not grow, and the organism instead executes a stepwise developmental process that culminates in the formation of multicellular dome-shaped aggregates called fruiting bodies. When development is completed, the swarm's millions of cells are parsed into fruiting bodies of $\sim 1 \times 10^5$ cells, a subset of which have differentiated to become metabolically quiescent and environmentally resistant myxospores located in the center. Development requires control of cell movement, division, and differentiation, as well as coordination and communication between cells and with the environment. Clp/Hsp100 proteins are good candidates for involvement in any or all of these processes.

MATERIALS AND METHODS

Cell cultivation and development. *M. xanthus* strains were grown at 32°C in CTTYE broth (1.0% Casitone, 0.5% yeast extract, 10 mM Tris-HCl [pH 8.0], 1 mM KH_2PO_4, and 8 mM $MgSO_4$) or on plates containing CTTYE broth and 1.5% agar (Difco). CTTYE broth and plates were supplemented with kanamycin (Kan) sulfate (20 and 40 μg/ml, respectively) as needed. For starvation-induced development, cells were spotted on TPM agar (10 mM Tris-HCl [pH 8.0], 1 mM KH_2PO_4, 8 mM $MgSO_4$, and 1.5% agar) at 32°C for 5 days. For glycerol-induced microcysts, *M. xanthus* cells were grown at 32°C to 5×10^8 cells/ml, and then glycerol was added to reach a final concentration of 0.5 M. Cell cultures were continuously shaken at 32°C over 8 h and then harvested for analysis.

In-frame deletion. DK1622Δ4832 (here referred to as "Δ4832") is a derivative of wild-type strain DK1622 that carries a 2,343-bp in-frame deletion of the MXAN_4832 gene locus. To create the deletion, a 4,602-bp fragment containing the MXAN_4832 gene locus and flanking DNA was generated by PCR using primers 4832_IFfw (5′-GAAGGGCATCTTGTC CAGCAGG-3′) and 4832_IFrv (5′-CTTCGATGGTCGTCACCGAGTG-3′). The 4,602-bp fragment was ligated into the pCR2.1-TOPO plasmid (Invitrogen), yielding plasmid pJY1 (Table 1). To generate plasmid pJY2, pJY1 was digested with EcoRI, and the 4,620-bp fragment containing MXAN_4832 and flanking DNA was ligated into EcoRI-digested pBJ114, a plasmid carrying the genes conferring kanamycin resistance (Kan^r) and galactose sensitivity (*galK* [Gal^s]), which is used for counter selection (33). An inverse PCR was performed using plasmid pJY2 and primers 4832_pBJ114_up (5′-TGA*CATCGAT*CATCTCGGGCGACATCCATGA GAACAG-3′) and 4832_pBJ114_dn (5′-GCCT*ATCGAT*TCCTCGTCTC CGAAGTCACTGAAGAAC-3′), each of which contains a ClaI digestion site (shown in italics). The PCR product was digested with ClaI, and the ClaI-digested DNA was treated with DNA ligase to generate plasmid pJY3. Plasmid pJY3, which carries the 2,343-bp in-frame deletion of the MXAN_4832 gene locus and flanking DNA, was then electroporated into *M. xanthus* cells to produce Kan^r transformants containing a single integration of pJY3 in the *M. xanthus* chromosome. This single integration event yields a tandem duplication with one intact copy of MXAN_4832 and one copy of MXAN_4832 carrying an in-frame deletion. After counter selection, Gal^r Kan^s cells that had lost pJY3 and carried the in-frame deletion of MXAN_4832 were identified using a pair of primers upstream

Received 8 November 2011 Accepted 18 January 2012
Published ahead of print 27 January 2012
Address correspondence to Roy D. Welch, rowelch@syr.edu.

doi:10.1128/JB.06492-11

TABLE 1 Strains and plasmids used in this study

Strain or plasmid	Relevant characteristic(s)[a]	Source or reference
Strains		
DK1622	Wild-type development	14
DK1218	DK1622, *tgl* (A^-S^+)	13
DK1253	DK1622, *cglB* (A^+S^-)	13
DK1622::pJY3	Strain with pJY3 inserted at the MXAN_4832 locus	This study
Δ4832	MXAN_4832 in-frame deletion	This study
RW10210	DK1622 with plasmid insertion at *pilI* locus	Unpublished data
Plasmids		
pCR2.1-TOPO	Kan^r	Invitrogen
pBJ114	Kan^r, *galK*	33
pGEX-4T-3	Amp^r, GST tag, thrombin cleavage site	GE Healthcare
pJY1	pCR2.1-TOPO with a 4,602-bp fragment containing MXAN_4832 locus and 2-kb flanking areas	This study
pJY2	pBJ114 with MXAN_4832 locus with 2-kb flanking areas	This study
pJY3	pJY2 with elimination of internal 2343 bp of MXAN_4832	This study
pJY4	MXAN_4832 whole gene locus in pGEX-4T-3	This study

[a] Kan^r, kanamycin resistance; Amp^r, ampicillin resistance.

and downstream of the MXAN_4832 gene locus (5′-TTCTGGGCGTAG TCGAGGAC-3′ and 5′-GGAAGAGATGGCTGCATCACG-3′). The mutant can generate a 722-bp fragment, while DK1622 fails to do so. In order to exclude the possibility of a mixed culture containing both Δ4832 and DK1622, the primer pair 5′-CGAGCTGGGACATTCCTATGTG-3′ and 5′-CTCGTCGATGAAGAGGACGATG-3′ was used to amplify part of the deleted region; a 535-bp fragment can be amplified in DK1622 but not in Δ4832.

Swarm and development phenotype assays. *M. xanthus* cells were grown with shaking in CTTYE broth and harvested at 5×10^8 cells/ml. For the swarm assay, cells were washed once with CTTYE and resuspended to a concentration of 5×10^9 cells/ml. Four spots of 2 μl of cells each were placed on CTTYE plates containing either 0.4% or 1.5% agar. Plates were incubated at 32°C for 3 days, after which swarm expansion was measured as a change in diameter versus time. For the aggregation assay, cells were washed once with TPM and resuspended to a concentration of 5×10^9 cells/ml. Between 5 and 10 spots of a 20-μl cell suspension were then spotted on TPM agar plates, allowed to dry, and incubated at 32°C. The formation of aggregates was observed and recorded at regular time intervals using 40× bright-field microscopy (Nikon) and SPOT imaging software (Diagnostic Instruments). For the sporulation assay, cells were prepared as described for the aggregation assay, and 20 μl was spotted on TPM agar and incubated at 32°C for 5 days to allow completion of development. Three groups of five spots each were harvested and suspended in 500 μl of TPM buffer. Cells were then exposed to a mild sonication (MISONIX S-4000 sonicator) (10% of maximum output, three times at 10 s each time with 30-s intervals) followed by heat treatment at 50°C for 2 h. Cells then were diluted to the desired concentration in CTTSA (1.0% Casitone, 10 mM Tris-HCl [pH 8.0], 1 mM KH_2PO_4, 8 mM $MgSO_4$, 0.7% agar) and plated onto CTTYE agar plates. After 5 days of incubation at 32°C, viable spores germinated and grew into visible colonies, and the number of colonies was recorded and converted to units of cells per milliliter.

***M. xanthus* swarm microcinematography.** Phase-contrast time-lapse microcinematography was used to record the movement of cells in a *M. xanthus* swarm. The ~1-mm-thick agar disks were formed in the wells of silicone gaskets on microscope slides. Cells were harvested at 5×10^8 cells/ml, washed once in CTTYE, and concentrated to 2.5×10^9 cells/ml, and then 2 μl was spotted onto one of the agar disks (1% agar–0.1% CTTYE). The cell droplet was allowed to dry before the disk was covered to prevent evaporation. The covered slide was then placed on a microscope stage heated to 32°C, and the swarm was monitored using phase-contrast microscopy at ×100 magnification. Images were recorded each minute over 24 h (Diagnosic Instruments) and stacked sequentially using QuickTime (Apple).

Agglutination assay. The agglutination assay was adapted from Wu et al. (39) and Arnold and Shimkets (2). Agitating cultures of *M. xanthus* in CTTYE were stopped during exponential growth at 5×10^8 cells/ml, and then turbidity was measured spectrophotometrically at time intervals for a total of 6 h as the cells clumped and settled out of the suspension. The absorbance at an optical density of 600 nm (OD_{600}) was measured using a Bio-mini (Shimadzu) spectrophotometer at every time interval. The initial absorbance was normalized to 100%, and every value was compared to the initial turbidity.

Calcofluor white binding assay. The assay was adopted from Yang et al. (41). *M. xanthus* cells were harvested at 5×10^8 cells/ml, pelleted, and then resuspended to a concentration of 5×10^7 cells/ml in CTTYE broth. A 10-μl aliquot of this cell suspension was then spotted on 1.5% CTTYE agar plates with calcofluor white (50 μg/ml). After the plate was incubated for 7 days at 32°C, pictures were taken using long-wavelength UV light.

Congo red binding assay. The Congo red binding assay was adopted from Weimer et al. (34). *M. xanthus* cells were harvested at 5×10^8 cells/ml, pelleted, and then resuspended in 2 ml of agglutination buffer (10 mM morpholinepropanesulfonic acid [MOPS], 1 mM $MgCl_2$, 1 mM $CaCl_2$ [pH 6.8]) (2) to a final concentration of 5×10^8 cells/ml. For the binding reaction, 1 ml of cell solution was transferred to a disposable cuvette, mixed with 20 μl of Congo red solution (2 mg/ml in agglutination buffer), and incubated at room temperature for 30 min. A control reaction was set up using the same cell strain with 20 μl of agglutination buffer and without Congo red. Reactions were scanned over a wavelength range of 400 to 700 nm using a Bio-mini spectrophotometer (Shimadzu). The final Congo red binding curve was obtained by subtracting the control baseline value from the binding reaction value. The absorption of Congo red alone was measured using a mixture of 20 μl of Congo red with 1 ml of agglutination buffer.

Fibril extraction. The procedure for extracting fibrils was performed as previously described (4, 7). Briefly, DK1622 cells were harvested at 5×10^8 cells/ml, and 3×10^9 cells were spread onto a 1.0% CTTYE agar plate. After incubation at 32°C for 3 days, cells were scraped and resuspended in 10 ml of ice-cold TNE (10 mM Tris, 100 mM NaCl, 5 mM EDTA, pH 7.5) buffer (4) and sonicated (10% output three times at 10 s each time) at 4°C and then 10 ml of TNE buffer containing 1% sodium dodecyl sulfate (SDS) was added. The cell suspension was stirred for 1 h at room temperature until the solution became clear. The cell lysate was centrifuged at $12{,}000 \times g$ for 10 min at 4°C to remove the supernatant. The solution was resuspended in 20 ml of TNE buffer with 0.5% SDS, stirred at room temperature for 1 h, and centrifuged at $12{,}000 \times g$ for 10 min at 4°C. This wash step was repeated twice, at which point there was no yellow pigment in the pellet. The pellet was then washed twice in 10 ml of TNE and centrifuged at $12{,}000 \times g$ for 10 min to remove SDS and then twice more in 10 ml of agglutination buffer to remove EDTA. Finally, the pellet was resuspended in 5 ml of agglutination buffer and stored at −20°C. The concentration of fibrils was determined as the content of carbohydrates by the use of a phenol-sulfuric acid assay (10).

Extraction of pili and Western blots of PilA protein. Cell surface pili were isolated from both Δ4832 and DK1622 cells as described previously (37). The RW10210 mutant strain was included as a control; RW10210 includes a deletion-disruption of the *pilI* gene that results in a strain that

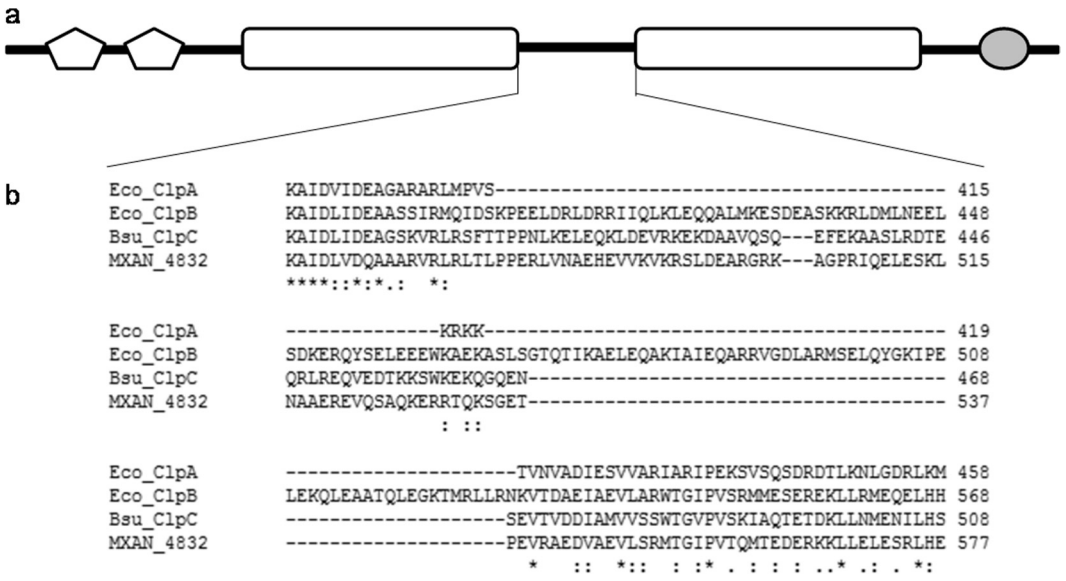

FIG 1 Sequence comparison of MXAN_4832 to Clp/Hsp100 proteins. (a) Diagram of MXAN_4832 protein domains. The two pentagons represent two ClpN domains, followed by two AAA domains drawn as rectangular open bars. The gray oval ClpB D2-small domain is located in the C terminus of the protein. The rest of the protein is represented with a thin black line. The picture is not drawn to scale. (b) Alignment of sequences around the linker regions among four ClpA, -B, and -C homologs based on BLASTP. Eco, *Escherichia coli*; Bsu, *Bacillus subtilis*. The length of this linker region is used to distinguish between ClpA, -B, and -C (32). MXAN_4832 and *B. subtilis* ClpC have similar linker region sizes.

can produce but does not export pili (Table 1). Therefore, RW10210 serves as a control for both the antibody and the isolation protocol for surface pili. The anti-PilA antibody (37) (provided by Mitch Singer) was diluted 1:1,000 and detected using an Immun-Star goat anti-rabbit (GAR)-horseradish peroxidase (HRP) detection kit (Bio-Rad).

Recombinant protein expression and purification. The entire MXAN_4832 open reading frame (ORF) was amplified using primers 4832AMfw (5′-GCAAGG*GTCGAC*ATGGCCAATGTCTGCGACCTCT GC-3′) and 4832AMrv (5′-ATAT*GCGGCCGC*TCAGTGAACGGCACT CGCTTCAGC-3′) with High Fidelity *Taq* DNA polymerase (Invitrogen) (italics indicate the SalI and NotI digestion sites). The resulting amplicon was digested with NotI and SalI and then ligated into NotI- and SalI-digested pGEX-4T-3 (GE Healthcare Life Sciences) to generate plasmid pJY4. Plasmid pJY4, which carries an MXAN_4832 fusion to glutathione *S*-transferase (GST), was introduced into BL21 Star(DE3) cells (Invitrogen), and these were grown at 25°C in LB supplemented with 2% glucose and ampicillin (50 mg/ml). When cell cultures reached an OD_{600} of 0.6 to 0.8, isopropyl-β-D-thiogalactopyranoside (IPTG) was added to reach a final concentration of 1 μM to induce protein expression, and the cell culture was shaken at 25°C for 24 h. The GST-MXAN_4832 fusion protein was purified using a GSTrap FF 5-ml column as described by the manufacturer (GE Healthcare Life Sciences). A thrombin CleanCleave kit (Sigma) was used to cleave the GST tag, and GST was removed from the MXAN_4832 protein suspension by the use of GSTrap FF (GE Healthcare Life Sciences). MXAN_4832 was concentrated using an Amicon Ultra-50 k (Millipore) centrifugal filter device. During each phase of the purification process, the protein samples were analyzed using SDS-polyacrylamide gel electrophoresis (SDS-PAGE).

Luciferase analysis. Recombinant luciferase and assay reagents were purchased from Promega, and active chaperones DnaK, DnaJ, and GrpE (KJE) were purchased from StressGen. The final protein concentrations in these assays were as follows: 1 mM MXAN_4832, 0.5 mM DnaK, 0.25 mM DnaJ, 0.25 mM GrpE. The procedure for the luciferase reactivation assay was adapted from those described previously (26, 35). Briefly, luciferase was incubated in refolding buffer (25 mM HEPES, 50 mM KCl, 5 mM Mg acetate, 5 mM β-mercaptoethanol, 10 μM ATP, pH 7.6) with or without MXAN_4832 and/or KJE. After equilibration to room temperature, the mixture was incubated at 42°C for 10 min. For the zero time point, 4 μl of the mixtures was removed immediately after heat treatment. The remainder of the reaction mixtures was then shifted to 25°C. After 10, 30, 60, 90, 120, and 180 min of incubation, 4 μl of reaction mixture was added to 200 μl of luciferase assay detergent. The mixtures were immediately transferred to cuvettes, and luciferase luminescence was measured at 562 nm using a QuantaMaster spectrofluorometer (PTI). The level of luminescence peaks within the first minute following the transfer of a reaction mixture to the luciferase assay detergent. Therefore, to ensure that the maximum level of luminescence was measured for each time point, luminescence was measured for 60 s at a frequency of 1 point per s immediately after the transfer of the reaction mixture to the luciferase assay detergent. Five continuous points that were in the peak of light illumination were selected, and the average energy of these points was calculated and used to represent the activity of luciferase.

RESULTS

MXAN_4832 is a homolog to ClpC/Hsp100 proteins. There are 12 open reading frames (ORFs) identified as Clp/Hsp100 homologs in the current annotation of the *M. xanthus* genome (GenBank accession no. NC_008095); from these, we selected MXAN_4832, because it is specifically a homolog of ClpC. We focused on a ClpC homolog because, in *B. subtilis*, a ClpC deletion significantly reduces endospore formation at 45°C (~1,000-fold compared to the *clpC*$^+$ strain) (22). We therefore hypothesized that a mutation in MXAN_4832 might exhibit a mutant sporulation phenotype in *M. xanthus* that involved a decreased resistance to heat. We also selected MXAN_4832 because ClpC homologs are rare in Gram-negative bacteria such as *M. xanthus*, suggesting that MXAN_4832 may have an important function.

Our annotation of MXAN_4832 as a Clp/Hsp100 homolog is based on five conserved domains (Fig. 1a). Alignment of MXAN_4832 with other identified ClpA, -B, and -C proteins reveals that the linker domain of MXAN_4832 is closest to ClpC (Fig. 1b). The function of the linker is not known, but its length is

used as an identifier to distinguish between ClpA, -B, and -C proteins (32).

Deletion of MXAN_4832 has no growth defect but reduces the swarm expansion rate. To study the cellular function of MXAN_4832, we constructed strain Δ4832 by counterselection (33). In an agitating liquid culture, Δ4832 shows no growth defect. In fact, its doubling time is slightly higher than that of wild-type DK1622 (~5%). It also reaches a slightly higher concentration before entering the stationary phase (~10%) (data not shown).

On an agar substrate, *M. xanthus* employs two genetically separable motility systems, called the adventurous (A-motility) and social (S-motility) systems. A swarm exhibiting only A-motility has a reduced rate of expansion on 0.4% (soft) agar compared to DK1622, and a swarm of cells exhibiting only S-motility has a reduced rate of expansion on 1.5% (hard) agar (15, 28). A comparison of mutant swarm expansion rates on both hard and soft agar can indicate a possible defect in one or both of these motility systems. Δ4832 has a reduced expansion rate on soft agar (~57.5% of the DK1622 rate) and a normal expansion rate on hard agar, indicating that its S-motility may be impaired.

To observe how Δ4832 differs from DK1622 with respect to the movement of cells within a swarm, we focused on cells at the swarm edge. Within a swarm, the A- and S-motility systems work synchronically, and the effect of each one can be observed at the edge of a swarm by the use of phase-contrast microscopy. After only a few hours of growth and expansion on 0.1% CTTYE agar, the edge of a DK1622 swarm exhibited a combination of multicellular flares and individual cells (Fig. 2a). In contrast, a swarm possessing only the S-motility system had an edge with flares but almost no individual cells (Fig. 2b), whereas a swarm with only A-motility had many individual cells and diminished flares (Fig. 2c). The swarm edge of Δ4832 (Fig. 2d) appears much more like that of an A^+S^- swarm than that of either an A^+S^+ or A^-S^+ swarm.

Normal S-motility requires functional fibrils and pili (36, 41). To determine if a defect in either fibrils and/or pili might cause the reduced rate of swarm expansion observed in Δ4832, we first performed an agglutination assay (Fig. 3a). Pili and fibrils are required for normal clumping in nonagitating liquid culture, and so a reduced rate of decrease in absorbance is a further indication of a possible defect. Using this assay, we determined that the Δ4832 agglutination rate matches the DK1622 rate during the first hour but is reduced compared to that of DK1622 after 3 h. These data support the hypothesis that there is a defect in the production of fibrils and/or pili (39).

To determine if Δ4832 can produce pili and export them to the cell surface, we isolated surface pili and examined them by Western blotting. These data indicate that the production and export of pili in Δ4832 are similar to those in DK1622 (Fig. 3b). We then examined the pattern and composition of fibrils within a swarm by the use of calcofluor white and Congo red. Staining an expanding swarm with calcofluor white reveals the pattern of the underlying matrix, and fibrils form an important part of this matrix. Figure 3b shows the calcofluor white staining patterns for both DK1622 and Δ4832, together with those of mutant strains DK1253 and DK1218, which have known S- and A-motility defects, respectively. The Δ4832 staining pattern is not like the DK1622 pattern, as it lacks the bright center around the area of the initial swarm, but staining was observed in Δ4832, which indicates that fibrils were being produced. In addition, the staining pattern

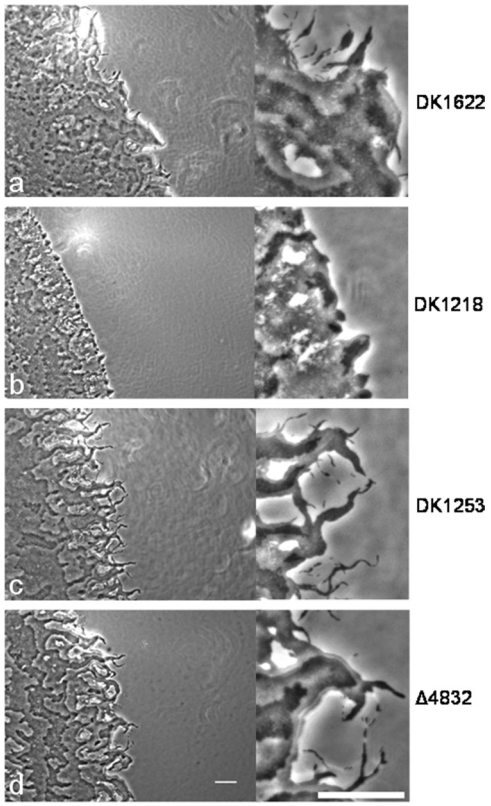

FIG 2 Swarm edges of Δ4832 motility mutants. Representative images were taken from microcinematography image stacks and were from h 2 after the initiation of swarming (white bar = 0.1 mm).

of Δ4832 does not appear similar to that of either DK1253 or DK1218, which indicates that the difference observed between Δ4832 and DK1622 is not simply due to the absence of one of the motility systems. What these observations do reveal is a possible defect in the timing of fibril production, since the area that binds to calcofluor white in Δ4832 can be seen only at the swarm edge.

We then used Congo red staining to determine if Δ4832 produces an abnormal amount of fibrils or if its fibrils have a different composition compared to those of DK1622. Congo red stains fibrils; upon staining, it shifts its absorbance spectrum. When the same numbers of Δ4832 and DK1622 cells are stained, the overall absorption reflects the amount of fibrils produced, and any shift in the absorption profile reflects a difference in fibril compositions. Figure 3c shows representative spectra for both Δ4832 and DK1622; the intensity of absorption is lower for Δ4832, but there is no shift in the absorption peak. These data indicate that Δ4832 produces fewer fibrils than DK1622 but that the Δ4832 fibrils that are produced are normal in composition.

Δ4832 exhibits defects in aggregation. When the cells were spotted on starvation TPM agar, Δ4832 aggregation was delayed by up to 36 h compared to that of DK1622, and the aggregates that did form were translucent and amorphous (Fig. 4a). To test if the delay in aggregation was due to the observed defects in the production of extracellular matrix, we examined the developmental impact of mixing Δ4832 cells either with DK1622 cells (which produce normal amounts of extracellular matrix) or with fibrils that had been extracted from DK1622 cells. Previous work showed

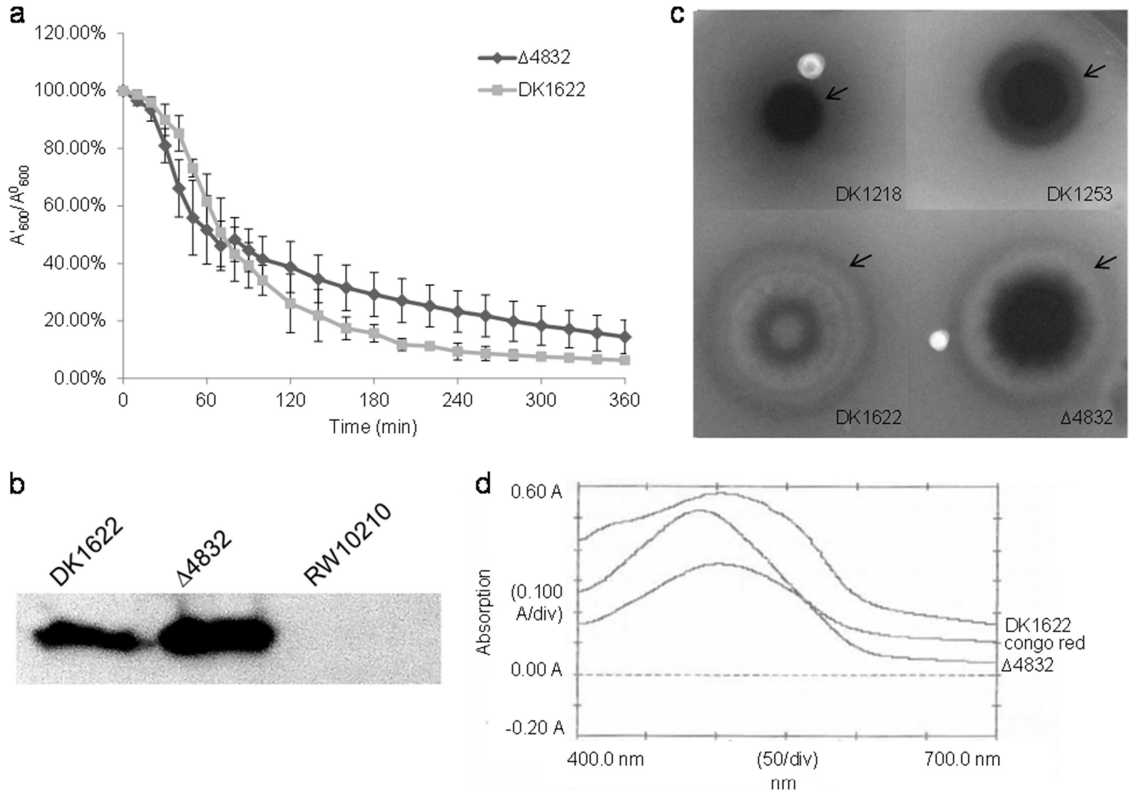

FIG 3 Test of extracellular matrix of Δ4832. (a) Agglutination assay. The absorbances of DK1622 and Δ4832 were checked every 10 min for the first 100 min and every 20 min for the remainder of the assay. Each strain was tested three times independently, and error bars show the standard deviation. (b) An immunoblot showing extracellular PilA. The third lane from the left represents RW10210, which is a mutant strain with an insertion in the *pilI* gene, an ABC transporter component required for exporting PilA. Thus, RW10210 does not have extracellular pili and serves as a negative control. (c) Calcofluor white binding of a Δ4832 swarm compared to DK1622 (A^+S^+), DK1253 (A^+S^-), and DK1218 (A^-S^+) swarms. Images were acquired with long-wavelength UV light. Arrows indicate the edges of colonies. (d) Spectrum scanning of Δ4832 binding with Congo red compared to DK1622 cells. The absorbance peak of Δ4832 does not shift but is lower than the peak of DK1622.

that fibrils from wild-type cells can rescue the aggregation morphology of a Dsp mutant, which lacks extracellular fibrils (6), and that this rescue can also be accomplished by mixing wild-type cells with Dsp mutant cells (29). We hypothesized that, if the aggregation delay of Δ4832 was due to a deficiency in fibrils, it also could be rescued by similar means. When DK1622 cells were mixed with Δ4832 cells in a 1:4 ratio, aggregation began within 24 h, and aggregates matured into elongated shapes (Fig. 4b). The efficiency of rescue was improved by increasing the proportion of DK1622 cells. A 1:1 (DK1622/Δ4832) ratio produced aggregates by h 12, with a morphology similar to that seen with 100% DK1622, and the results produced by a 2:1 ratio were almost indistinguishable from the 100% DK1622 results.

We have already observed that Δ4832 produces both fibrils and pili, but perhaps one or both are not able to function properly. To test whether the observed aggregation defects in Δ4832 might be related to its pili, we performed a rescue experiment using extracellular pili isolated from DK1622 cells. Aggregation of Δ4832 can be rescued by isolated pili from the same number of DK1622 cells within 24 h (Fig. 4c), and the aggregates are darker and have more distinct edges than Δ4832 cells without DK1622 extract. Interestingly, isolated pili from Δ4832 were also able to slightly rescue Δ4832 aggregation, but the DK1622 extract was much more effective (Fig. 4c). To test the hypothesis that fibrils from DK1622 are responsible for the whole-cell rescue of Δ4832 aggregation, we extracted fibrils from DK1622 cells and then added them to Δ4832 cells prior to starvation. This extract is able to rescue Δ4832 aggregation, and when added to a final concentration of a 1 mg/ml equivalent of carbohydrates, the resulting aggregates were very similar to those seen with DK1622 (Fig. 4d). Note that both the pili and the fibril extracts were enriched but not highly purified and therefore may have contained other factors that are also involved in aggregation. Nevertheless, when the results of these three rescue experiments are considered, they indicate that the aggregation defect in Δ4832 can be rescued by adding back an extracellular component enriched for pili and fibrils and therefore that pili and fibrils likely contribute to the aggregation mutant phenotype.

Δ4832 produces heat-sensitive spores. In a swarm of DK1622 cells, spores form within aggregates when development is nearly complete, which marks the transition from aggregates to mature fruiting bodies. Even though swarms of Δ4832 produce abnormal and delayed aggregates, the sporulation efficiency of Δ4832 is normal under standard assay conditions (50°C). These data are significant, because they indicate that the observed motility or aggregation abnormalities do not significantly impact the ability of Δ4832 to form spores. This finding is not unprecedented; mutations that produce motility and/or aggregation defects do not necessarily affect sporulation (38, 42). On the other hand, the standard sporulation assay represents only one set of conditions. Just because a mutant strain's spores are unaffected by those condi-

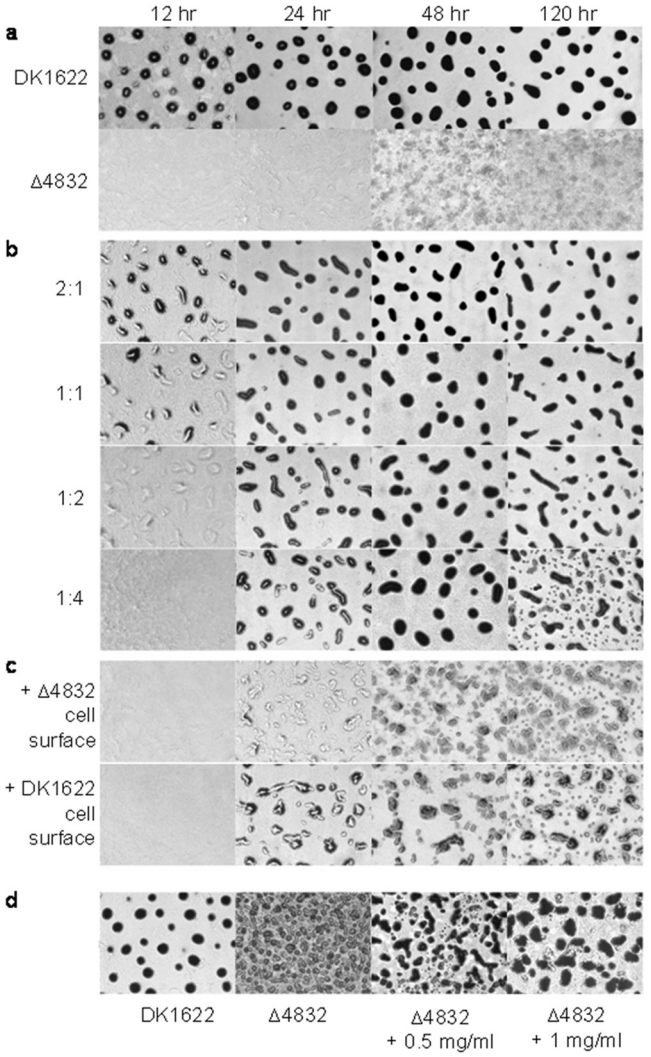

FIG 4 Aggregation assay and rescue experiments. Δ4832 displays delayed aggregation on TPM starvation agar. (a) Wild-type DK1622 shows obvious aggregation centers (black dots) at h 12 after starvation. Δ4832 forms aggregates by h 48, but they are less condensed, even at h 120. (b) Aggregation rescue of Δ4832 by DK1622 cells. The number in front of each row indicates the ratio of DK1622 cells to Δ4832 cells. The timing and shape of aggregates were dependent on the ratio of DK1622 cells. A 2:1 ratio exhibits aggregation similar to that seen with 100% DK1622. (c) Aggregation rescue of Δ4832 by isolated pili from Δ4832 cells (upper panel) and DK1622 cells (lower panel). (d) Aggregation rescue by DK1622 fibrils. Δ4832 cells restored aggregation when fibrils from DK1622 were added before starvation. Images were acquired at h 72 after development initiation.

tions, it does not prove that the spores are the same as those of DK1622.

If we alter the conditions slightly, the results of the Δ4832 sporulation assay data change significantly. The "standard" sporulation assay involves heating a suspension of cells from mature aggregates at 50°C to kill all cells that are not spores and then plating the suspension and eventually counting the colonies of emergent spores that survived. If we increase the heating temperature to 55°C instead of the standard 50°C, the sporulation efficiency of Δ4832 is reduced to less than 1% of the efficiency of DK1622 (Table 2). Therefore, although Δ4832 sporulation does not seem to have been impaired (Δ4832 forms approximately the same number of spores in the same amount of time as DK1622 based on the standard assay), the spores that were produced by Δ4832 during development were not the same as those of DK1622; they were more sensitive to heat.

To explore the relationship between Δ4832 development and the heat sensitivity of Δ4832 spores, we tested the heat resistance of Δ4832 spores that were created using an alternative mechanism of sporulation that is partly decoupled from development. *M. xanthus* cells can also be induced to form spores by exposing them to glycerol. This process is comparatively rapid and bypasses some of the developmental process (9). Interestingly, the Δ4832 glycerol-induced spores displayed heat sensitivity similar to that of DK1622 spores at both 50°C (data not shown) and 55°C (Table 2), indicating that the difference we observed between Δ4832 and DK1622 starvation-induced spores was due to something that occurs (or does not occur) during the process of development rather than to some inherent inability of Δ4832 cells to become spores.

MXAN_4832 functions as a molecular chaperone *in vitro*. Δ4832 exhibits defects similar to those of Clp/Hsp100 mutants in other bacteria, but can the protein product of MXAN_4832 function as a chaperone? To test this, we performed an *in vitro* biochemical characterization using a luciferase reactivation assay. At 25°C, luciferase catalyzes the oxidation of luciferin and produces luminescence at a wavelength of 562 nm. This reaction is sensitive to heat, and luciferase is permanently inactivated when heated to 42°C. Clp/Hsp100 proteins can prevent this permanent inactivation if and only if the purified protein is added prior to heating (1, 35). When it is, then luciferase can be refolded through the addition of molecular chaperones DnaK, DnaJ, and GrpE (KJE) (StressGen) (1, 26, 27, 35). To determine if the protein product of MXAN_4832 can function as a chaperone, we tested its ability to prevent the permanent inactivation of luciferase.

In our assay, the *E. coli* chaperone set KJE, as well as MXAN_4832, was added to the reaction before and/or after the heat shock treatment. KJE would recover luciferase activity only if it were present before heat shock (35), which was also confirmed in our assay (Fig. 5, diamonds). Substituting MXAN_4832 for KJE before heat shock restored some of the activity when KJE was added after heat shock (Fig. 5, light squares). When MXAN_4832 was absent before heat shock (Fig. 5, triangles), or when KJE was not added after heat shock (Fig. 5, dark squares), then luciferase was not reactivated. We therefore conclude that MXAN_4832 can function to protect luciferase from permanent inactivation and is therefore a chaperone.

DISCUSSION

Here we report the phenotypic and biochemical characterization of MXAN_4832 in *M. xanthus*; it is the first Clp/Hsp100 ortholog

TABLE 2 Spore assay of DK1622 and Δ4832 with heat treatment

Strain	Avg % ± SE at indicated temp[a]		
	Fruiting body spores		Glycerol spores (55°C)
	50°C	55°C	
DK1622	100 ± 5.87	100 ± 13.53	100 ± 30.21
Δ4832	164.42 ± 21.31	0.50 ± 0.04	92.01 ± 36.48

[a] Percentage data are shown as averages ± standard errors. The assay was independently repeated in triplicate at least three times.

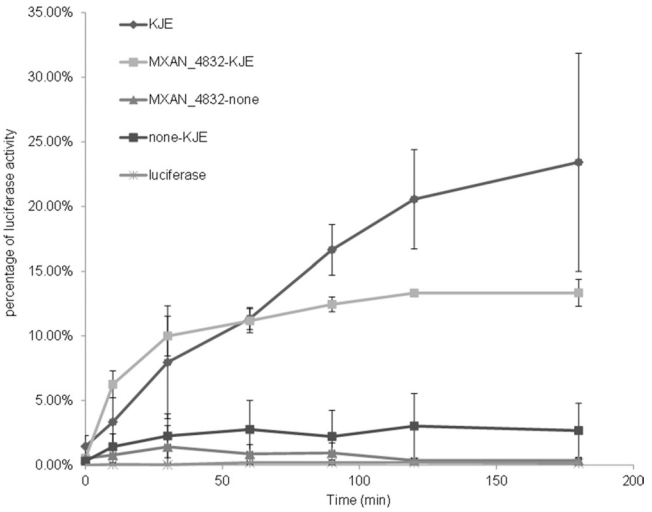

FIG 5 Luciferase reactivation assay of MXAN_4832 protein. Luciferase incubated with *E. coli* KJE heat shock proteins before heat shock (diamonds) can recover up to 20% of the original activity. Luciferase incubated with MXAN_4832 protein before heat shock with additional KJE after heat shock can also recover more than 12% of the original activity (light squares). Without MXAN_4832 protein added before heat shock, KJE added after heat shock (dark squares) did not reactivate luciferase. Also, when no KJE was added to the heat-treated MXAN_4832-luciferase mixture, luciferase was not reactivated (triangles). Crosses indicate the activity of luciferase without any molecular chaperones. All experiments were repeated independently at least three times, and standard deviations are shown.

to be characterized in a myxobacterium. We demonstrate that deletion of MXAN_4832 in *M. xanthus* produces a mutant strain with a normal vegetative growth rate but with defects in swarming and aggregation. Agglutination assays, fluorescent staining, and rescue experiments all indicate that these defects could be due to changes in fibrils and/or pili within a swarm. These data are consistent with the results of motility assays and a qualitative analysis of the swarm edge, both of which indicate that the deletion disproportionately affects the S-motility system. Defects in fibrils have previously been linked to both S-motility and developmental abnormalities (18). In *M. xanthus*, fibrils regulate retraction of pili (18) and potentially contain receptors for attachment of pili (31). Also, fibrils contain receptors for chemical signals, such as dilauroyl phosphatidylethanolamine (PE) (16), which stimulates the chemotaxis receptor DifA under starvation conditions (5). To have an effect on S-motility and aggregation, MXAN_4832 does not need to directly coordinate multicellular behavior. Instead, it may function in related processes such as the biosynthesis, transportation, and maturation of fibrils or fibril-related proteins.

An analysis by Western blotting indicates that the production and export of pili are not impaired in Δ4832 but that Δ4832 aggregation can be rescued by adding isolated extracellular pili from either DK1622 or Δ4832 (although DK1622 is much more effective). This may mean that the pili in Δ4832 do not function as well as those in DK1622, but that is only one of several plausible interpretations. For example, the preparation of isolated pili may contain other cell surface components, such as fibrils or peptidoglycan, and thus the observed rescue by isolated DK1622 and Δ4832 pili may actually be related to the production of fibrils. It is also possible that peptidoglycan might be involved, since peptidoglycan components have been found to induce rippling in wild-type cells and rescue certain sporulation mutants such as *csgA* (30). Although no direct relationship has been established between cellular peptidoglycan and cell aggregation, it could be a factor that contributes to the observed Δ4832 aggregation phenotype.

The delayed, translucent, and amorphous aggregates formed by Δ4832 during development appear very different from those formed by DK1622, but they produce a normal number of spores, and these survive the "standard" sporulation assay conditions that kill vegetative cells. Our finding that a further increase in temperature to 55°C is required for the difference between Δ4832 and DK1622 spores to become apparent is a further indication that Δ4832 can make nearly normal spores but that these spores are sensitive to heat. The fact that a heat-sensitive sporulation phenotype is observed in a ClpC deletion strain of *B. subtilis* is interesting and indicates that ClpC is important for the formation of both endospores and myxospores. Our observation that glycerol-induced Δ4832 spores are not heat sensitive indicates that the defect occurs during the process of starvation-induced development and that it weakens but does not interrupt Δ4832 sporulation.

Finally, we demonstrate that the protein product of MXAN_4832 can function as a chaperone *in vitro*, thus supporting our hypothesis that it is a functional ClpC ortholog. There is evidence that ClpC orthologs also function in other biofilm-forming species. For example, deletion of ClpC impairs biofilm formation in *Staphylococcus aureus* (11), and ClpC expression is induced in both *S. aureus* and *Leptospirillum* spp. in the filamentous biofilm (3, 19). From our experimental results, we propose that MXAN_4832 impacts an *M. xanthus* biofilm through the timing and distribution of fibrils. There is precedence for such a model; another molecular chaperone identified in *M. xanthus*, MXAN_6671, is a DnaK ortholog that was found to mediate production of fibrils (34, 40). Deletion of MXAN_6671 results in an absence of fibrils and severe developmental defects (34, 40). It is possible that the functional pathways of DnaK and MXAN_4832 overlap in *M. xanthus* fibril production.

ACKNOWLEDGMENTS

We thank Robert Doyle for generously providing the protein expression vector and protein purification system as well as kindly giving advice, Bruce Hudson for advice in the luminance assay and for providing the QuantaMaster equipment, Mitch Singer for providing the anti-PilA antibody, and Laura Welch for generously helping edit our manuscript.

This work was supported primarily by National Science Foundation (NSF) Career award MCB-0746066 to R. D. Welch and NSF grant IOS-0950976 to A. G. Garza.

REFERENCES

1. **Andersson FI, et al.** 2006. Cyanobacterial ClpC/HSP100 protein displays intrinsic chaperone activity. J. Biol. Chem. **281**:5468–5475.
2. **Arnold JW, Shimkets LJ.** 1988. Inhibition of cell-cell interactions in *Myxococcus xanthus* by Congo red. J. Bacteriol. **170**:5765–5770.
3. **Becker P, Hufnagle W, Peters G, Herrmann M.** 2001. Detection of differential gene expression in biofilm-forming versus planktonic populations of *Staphylococcus aureus* using micro-representational-difference analysis. Appl. Environ. Microbiol. **67**:2958–2965.
4. **Behmlander RM, Dworkin M.** 1991. Extracellular fibrils and contact-mediated cell interactions in *Myxococcus xanthus*. J. Bacteriol. **173**:7810–7820.
5. **Bonner PJ, et al.** 2005. The Dif chemosensory pathway is directly involved in phosphatidylethanolamine sensory transduction in *Myxococcus xanthus*. Mol. Microbiol. **57**:1499–1508.
6. **Chang BY, Dworkin M.** 1994. Isolated fibrils rescue cohesion and development in the Dsp mutant of *Myxococcus xanthus*. J. Bacteriol. **176**:7190–7196.

7. **Clemans DL, Chance CM, Dworkin M.** 1991. A development-specific protein in Myxococcus xanthus is associated with the extracellular fibrils. J. Bacteriol. **173**:6749–6759.
8. **Dougan DA, Mogk A, Zeth K, Turgay K, Bukau B.** 2002. AAA+ proteins and substrate recognition, it all depends on their partner in crime. FEBS Lett. **529**:6–10.
9. **Dworkin M.** 1996. Recent advances in the social and developmental biology of the myxobacteria. Microbiol. Rev. **60**:70–102.
10. **Fournier E.** 2001. Colorimetric quantification of carbohydrates, p E1.1.1–E1.1.2. *In* Reid D (ed), Current protocols in food analytical chemistry. Wiley, Hoboken, NJ.
11. **Frees D, et al.** 2004. Clp ATPases are required for stress tolerance, intracellular replication and biofilm formation in *Staphylococcus aureus*. Mol. Microbiol. **54**:1445–1462.
12. **Gottesman S, Maurizi MR, Wickner S.** 1997. Regulatory subunits of energy-dependent proteases. Cell **91**:435–438.
13. **Hodgkin J, Kaiser D.** 1979. Genetics of gliding motility in *Myxococcus xanthus*: two gene systems control movement. Mol. Gen. Genet. **171**:177–191.
14. **Kaiser D.** 1979. Social gliding is correlated with the presence of pili in *Myxococcus xanthus*. Proc. Natl. Acad. Sci. U. S. A. **76**:5952–5956.
15. **Kaiser D, Crosby C.** 1983. Cell movement and its coordination in swarms of *Myxococcus xanthus*. Cell Motil. **3**:227–245.
16. **Kearns DB, Campbell BD, Shimkets LJ.** 2000. *Myxococcus xanthus* fibril appendages are essential for excitation by a phospholipid attractant. Proc. Natl. Acad. Sci. U. S. A. **97**:11505–11510.
17. **Krüger E, Msadek T, Ohlmeier S, Hecker M.** 1997. The *Bacillus subtilis clpC* operon encodes DNA repair and competence proteins. Microbiology **143**:1309–1316.
18. **Li Y, et al.** 2003. Extracellular polysaccharides mediate pilus retraction during social motility of *Myxococcus xanthus*. Proc. Natl. Acad. Sci. U. S. A. **100**:5443–5448.
19. **Moreno-Paz M, Gomez MJ, Arcas A, Parro V.** 2010. Environmental transcriptome analysis reveals physiological differences between biofilm and planktonic modes of life of the iron oxidizing bacteria *Leptospirillum spp*. in their natural microbial community. BMC Genomics **11**:404.
20. **Nair S, Frehel C, Nguyen L, Escuyer V, Berche P.** 1999. ClpE, a novel member of the HSP100 family, is involved in cell division and virulence of *Listeria monocytogenes*. Mol. Microbiol. **31**:185–196.
21. **Nair S, Milohanic E, Berche P.** 2000. ClpC ATPase is required for cell adhesion and invasion of *Listeria monocytogenes*. Infect. Immun. **68**:7061–7068.
22. **Nanamiya H, et al.** 1998. ClpC regulates the fate of a sporulation initiation sigma factor, sigmaH protein, in *Bacillus subtilis* at elevated temperatures. Mol. Microbiol. **29**:505–513.
23. **Rouquette C, de Chastellier C, Nair S, Berche P.** 1998. The ClpC ATPase of *Listeria monocytogenes* is a general stress protein required for virulence and promoting early bacterial escape from the phagosome of macrophages. Mol. Microbiol. **27**:1235–1245.
24. **Rouquette C, et al.** 1996. Identification of a ClpC ATPase required for stress tolerance and in vivo survival of *Listeria monocytogenes*. Mol. Microbiol. **21**:977–987.
25. **Schirmer EC, Glover JR, Singer MA, Lindquist S.** 1996. HSP100/Clp proteins: a common mechanism explains diverse functions. Trends Biochem. Sci. **21**:289–296.
26. **Schlothauer T, Mogk A, Dougan DA, Bukau B, Turgay K.** 2003. MecA, an adaptor protein necessary for ClpC chaperone activity. Proc. Natl. Acad. Sci. U. S. A. **100**:2306–2311.
27. **Schröder H, Langer T, Hartl FU, Bukau B.** 1993. DnaK, DnaJ and GrpE form a cellular chaperone machinery capable of repairing heat-induced protein damage. EMBO J. **12**:4137–4144.
28. **Shi W, Zusman DR.** 1993. The two motility systems of *Myxococcus xanthus* show different selective advantages on various surfaces. Proc. Natl. Acad. Sci. U. S. A. **90**:3378–3382.
29. **Shimkets LJ.** 1986. Role of cell cohesion in *Myxococcus xanthus* fruiting body formation. J. Bacteriol. **166**:842–848.
30. **Shimkets LJ, Kaiser D.** 1982. Murein components rescue developmental sporulation of *Myxococcus xanthus*. J. Bacteriol. **152**:462–470.
31. **Spormann AM.** 1999. Gliding motility in bacteria: insights from studies of *Myxococcus xanthus*. Microbiol. Mol. Biol. Rev. **63**:621–641.
32. **Squires C, Squires CL.** 1992. The Clp proteins: proteolysis regulators or molecular chaperones? J. Bacteriol. **174**:1081–1085.
33. **Ueki T, Inouye S, Inouye M.** 1996. Positive-negative KG cassettes for construction of multi-gene deletions using a single drug marker. Gene **183**:153–157.
34. **Weimer RM, Creighton C, Stassinopoulos A, Youderian P, Hartzell PL.** 1998. A chaperone in the HSP70 family controls production of extracellular fibrils in *Myxococcus xanthus*. J. Bacteriol. **180**:5357–5368.
35. **Wickner S, et al.** 1994. A molecular chaperone, ClpA, functions like DnaK and DnaJ. Proc. Natl. Acad. Sci. U. S. A. **91**:12218–12222.
36. **Wu SS, Kaiser D.** 1995. Genetic and functional evidence that type IV pili are required for social gliding motility in *Myxococcus xanthus*. Mol. Microbiol. **18**:547–558.
37. **Wu SS, Kaiser D.** 1997. Regulation of expression of the *pilA* gene in *Myxococcus xanthus*. J. Bacteriol. **179**:7748–7758.
38. **Wu SS, Wu J, Cheng YL, Kaiser D.** 1998. The *pilH* gene encodes an ABC transporter homologue required for type IV pilus biogenesis and social gliding motility in *Myxococcus xanthus*. Mol. Microbiol. **29**:1249–1261.
39. **Wu SS, Wu J, Kaiser D.** 1997. The *Myxococcus xanthus pilT* locus is required for social gliding motility although pili are still produced. Mol. Microbiol. **23**:109–121.
40. **Yang Z, Geng Y, Shi W.** 1998. A DnaK homolog in *Myxococcus xanthus* is involved in social motility and fruiting body formation. J. Bacteriol. **180**:218–224.
41. **Yang Z, et al.** 2000. *Myxococcus xanthus dif* genes are required for biogenesis of cell surface fibrils essential for social gliding motility. J. Bacteriol. **182**:5793–5798.
42. **Zusman DR.** 1982. "Frizzy" mutants: a new class of aggregation-defective developmental mutants of *Myxococcus xanthus*. J. Bacteriol. **150**:1430–1437.